

# Enhanced Conductance Fluctuation by Quantum Confinement Effect in Graphene Nanoribbons

Guangyu Xu,<sup>\*,†</sup> Carlos M. Torres, Jr.,<sup>†</sup> Emil B. Song,<sup>†</sup> Jianshi Tang,<sup>†</sup> Jingwei Bai,<sup>†</sup> Xiangfeng Duan,<sup>§</sup> Yuegang Zhang,<sup>\*,||</sup> and Kang L. Wang<sup>†</sup>

<sup>†</sup>Department of Electrical Engineering, <sup>†</sup>Department of Material Science and Engineering, and <sup>§</sup>Department of Chemistry and Biochemistry, University of California at Los Angeles, Los Angeles, California 90095, United States and <sup>||</sup>Molecular Foundry, Lawrence Berkeley National Laboratory, 1 Cyclotron Road, Berkeley, California 94720, United States

**ABSTRACT** Conductance fluctuation is usually unavoidable in graphene nanoribbons (GNR) due to the presence of disorder along its edges. By measuring the low-frequency noise in GNR devices, we find that the conductance fluctuation is strongly correlated with the density-of-states of GNR. In single-layer GNR, the gate-dependence of noise shows peaks whose positions quantitatively match the subband positions in the band structures of GNR. This correlation provides a robust mechanism to electrically probe the band structure of GNR, especially when the subband structures are smeared out in conductance measurement.

**KEYWORDS** Graphene nanoribbon, quantum transport, low-frequency noise, electrical probing, band structure.

Considerable interest in mesoscopic low-dimensional electron systems has been motivated by a variety of unusual transport phenomena originating from the quantum confinement effect.<sup>1–3</sup> Inherent to quantum transport systems, enhanced conductance fluctuations due to disorder have brought intensive discussions on their correlation with the quantized density-of-states.<sup>4,5</sup> To date, research on conductance fluctuations is not only the subject of main scientific concerns in kinetics of quantum transport<sup>6,7</sup> but also of particular interest in probing the electronic band structure of low-dimensional nanostructures.<sup>8,9</sup> Low-frequency conductance fluctuation, or the flicker noise, has been broadly utilized to characterize the trap-induced charge switching processes.<sup>10,11</sup> The finding of strong correlation between the trap-induced conductance fluctuations (noise) and the density-of-states (DOS) in low-dimensional nanostructures has raised broad interest in the research of two-dimensional electron-gas (2DEG) and multiple cross-fields.<sup>9,12–15</sup>

Graphene has recently attracted much attention for its ultrahigh intrinsic carrier mobility and thermal conductivity, both of which greatly benefit device applications.<sup>16,17</sup> Graphene nanoribbon (GNR), the graphene with a nanometer-size width, is a quasi-one-dimensional (1D) material with the presence of an energy gap,<sup>18</sup> which is advantageous over the large graphene (no bandgap) for switching on/off the devices. However, the quantum transport of GNRs is still poorly understood: much debate remains on the origins of

the energy gap in GNR,<sup>19–22</sup> whereas the correlation of conductance fluctuations with the quantum confinement effect along the width of GNR has been amazingly unexplored. On the other hand, although previous works report the subband formation of GNR as indicated in the observation of quantized conductance plateaus,<sup>23,24</sup> these plateaus can be significantly disturbed by multiple types of disorder similar to the case in quantum wire systems.<sup>25–27</sup> A more robust and direct probing mechanism to the band structure of GNR is thus critical and of fundamental interest to examine the intrinsic electrical properties of GNRs. In this context, a recent work by Lin et al. showed the room temperature noise measurement of GNRs, which shed light on the noise dependence on the change of energy gap in bilayer GNRs.<sup>28</sup>

In this Letter, we report the observation of strong correlation between the enhanced conductance fluctuations of GNR and its electronic band structure. By measuring the low-frequency noise of GNR devices at low temperature (77 K), we find that the enhanced conductance fluctuations (noise) originate from the quantum confinement effect along the GNR widths: in single-layer GNR (SLR), the gate-dependence of noise shows peaks whose positions quantitatively agree with the quasi-1D transport theory; in bilayer GNR (BLR), the noise peaks are also obvious while the band structure is unclear in conductance data. The correlation between noise and DOS provides a robust mechanism to directly probe the band structure of GNRs, especially when the subband feature is smeared out in conductance measurement. Our result can extend to a broad range of low-dimensional nanostructures and reinvigorate interest toward implementing conductance

\* To whom correspondence should be addressed. E-mail: (G.X.) guangyu@ee.ucla.edu; (Y.Z.) yzhang5@lbl.gov.

Received for review: 07/24/2010

Published on Web: 10/12/2010



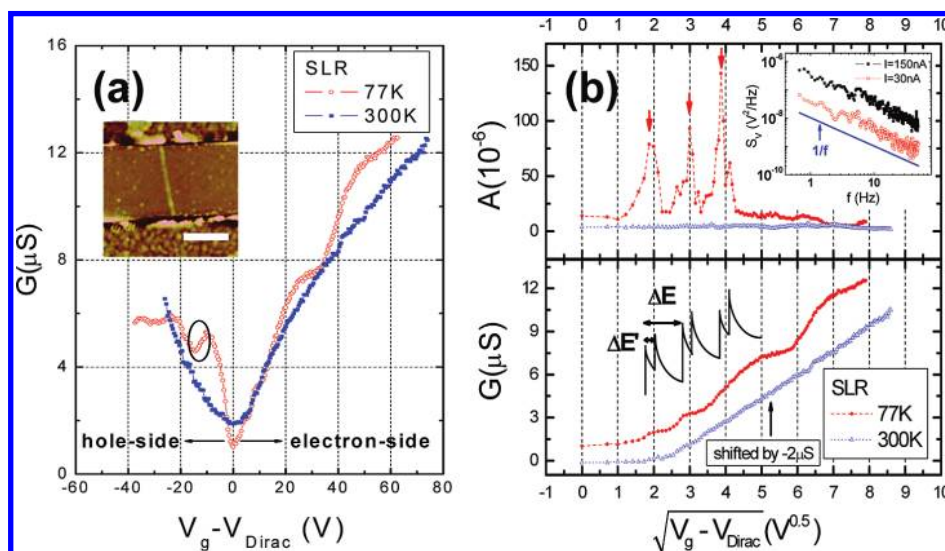


**FIGURE 1.** Temperature-dependence of noise behavior (and conductance) in single layer graphene nanoribbon (SLR). (a)  $T$ -dependent dc conductance ( $G$ ) versus gate bias ( $V_g - V_{\text{Dirac}}$ ) for SLR1 ( $W \sim 42$  nm,  $L \sim 0.81$   $\mu\text{m}$ ). The circled area shows negative differential conductance regime at 77 K. The inset shows the AFM image of the measured SLR1. The scale bar is equal to 0.5  $\mu\text{m}$ . (b)  $T$ -dependent noise ( $A$ , top) and conductance ( $G$ , bottom) in the electron-conduction side of SLR1 in scale of  $(V_g - V_{\text{Dirac}})^{1/2}$ . At  $T = 77$  K, the noise peaks (top) are shown to appear (not apparent at  $T = 300$  K) near the transition of the conductance plateaus (bottom) near the Dirac point (as arrowed), which suggest their correlation with the quasi-1D transport in SLR. Vertical dotted lines are guides to the eyes. The upper inset shows typical  $1/f$  noise spectra collected in SLR1, where the background noise measured at zero current bias has been subtracted. The solid line shows the normalized  $1/f$  noise scaled to  $S_v = 1 \times 10^{-8}$   $\text{V}^2/\text{Hz}$  at  $f \sim 1$  Hz. The bottom inset shows the schematics of quasi-1D DOS in scale of  $(V_g - V_{\text{Dirac}})^{1/2}$  (the K-K' subband splitting,  $\Delta E'$ , is not in scale).

fluctuations (noise) for fundamental studies of quantum transport systems.

GNR samples were prepared by a nanowire-mask-based fabrication method as reported before.<sup>29</sup> The GNRs were patterned into multiprobe structures by e-beam lithography. GNR devices were maintained in vacuum environment, and a vacuum bakeout process was applied to partially desorb contaminants before the measurements.<sup>21</sup> We apply a standard four-probe setup to reduce the noise contribution from the contacts:<sup>30</sup> an Agilent 4156C was used to apply dc current to the GNR within its linear regime; an Agilent 35670A was used to collect the noise spectra of the fluctuations in the potential difference (V) across the GNR sample. Under each gate bias ( $V_g$ ), the dc conductance ( $G$ ) and low-frequency noise spectra ( $S_v$ ) were collected at the same time to avoid the hysteresis effect (see Supporting Information). We use the frequency ( $f$ )-averaged noise figure  $A = (1/2) \sum_{i=1}^Z f_i \times S_{v_i}/V^2$  to characterize the noise level, where the noise spectra follow with a  $1/f^\alpha$  behavior ( $\alpha$  ranging from 0.85 to 1.12).<sup>31</sup> The dimension of GNR samples (the length ( $L$ ) and width ( $W$ )) are measured by detailed atomic-force-microscopy (AFM) scanning.<sup>29</sup>

Figure 1a shows the typical temperature ( $T$ )-dependent  $G$  versus  $V_g$  curves (shifted by the gate bias at Dirac point,  $V_{\text{Dirac}}$ ) for a SLR sample, where the electron-hole asymmetry may be caused by the contact-doping effect.<sup>32</sup> Because of quasi-1D subband formation, the conductance plateaus appear at  $T = 77$  K for both electron- ( $V_g - V_{\text{Dirac}} > 0$ ) and hole-conduction ( $V_g - V_{\text{Dirac}} < 0$ ) sides, and smear out at  $T = 300$  K.<sup>23</sup> The negative differential conductance region (i.e.,

$\partial G/\partial |V_g| < 0$  as circled) results from the enhanced intersubband scattering near the transition of conductance plateaus.<sup>27</sup>

To see the noise correlation with quasi-1D subband formation, we rescale the gate-dependence of the noise as  $(|V_g - V_{\text{Dirac}}|)^{1/2}$  in SLR and  $|V_g - V_{\text{Dirac}}|$  in BLR for the rest of this paper.<sup>33,34</sup> This representation helps show the noise behavior in the energy scale ( $E_{\text{SLR}} \sim (|V_g - V_{\text{Dirac}}|)^{1/2}$  and  $E_{\text{BLR}} \sim |V_g - V_{\text{Dirac}}|$ ), where the difference for SLR and BLR comes from their different energy dispersions.<sup>34</sup> We confirmed that the noise spectra follow  $1/f$  behavior (see top inset of Figure 1b) at each applied gate bias, thus the definition of noise figure ( $A$ ) is valid.<sup>9,28</sup>

Figure 1b shows the gate-dependence of the noise figure ( $A$ ) for electron-conduction side of SLR1 (the data for hole-conduction side are qualitatively the same). At  $T = 77$  K, the noise curves (top) show noise peaks near the transition of conductance plateaus (bottom). The main noise peaks (as arrowed) are nearly equidistant in the scale of  $(V_g - V_{\text{Dirac}})^{1/2}$ ; this is consistent with the fact that the separation of the quasi-1D subbands (see the bottom inset of Figure 1b) is nearly constant (the K-K' subband splitting effect is discussed in Figure 2).<sup>23,24,27</sup> The noise peaks are confirmed to be independent from the applied current, gate sweeping direction and frequency range, assuring that their origin comes from intrinsic trapping/detrapping processes near the SLR.

We propose that the noise peaks originate from the enhanced trap-induced conductance fluctuations that follow the density-of-states (DOS) of SLR (see bottom inset of Figure

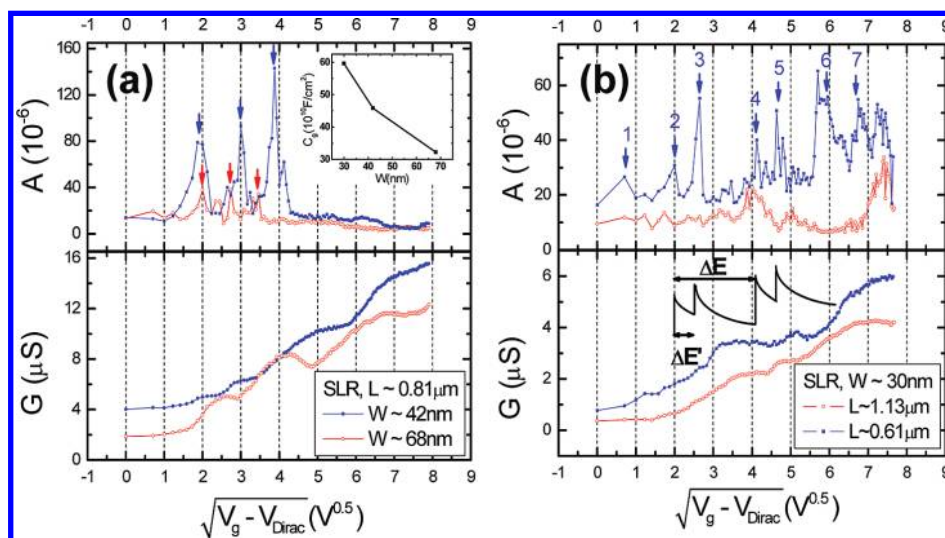


FIGURE 2. Dimension-dependence of noise behavior (and conductance) in single layer graphene nanoribbon (SLR). (a)  $W$ -dependence of noise behavior of SLR1 ( $W \sim 42$  nm) and SLR2 ( $W \sim 68$  nm) with a similar length ( $L \sim 0.81$   $\mu\text{m}$ ) at  $T = 77$  K in scale of  $(V_g - V_{\text{Dirac}})^{1/2}$ . As  $W$  increases, the separation of main noise peaks (as arrowed) near the Dirac point decreases. The inset shows the effective gate capacitance of SLRs,  $C_{\text{total}}$ , versus the width ( $W$ ) using the classical model of a conducting strip (infinitely long). The oxide thicknesses,  $t_{\text{ox}}$ , are measured as  $t_{\text{ox}}(W \sim 30$  nm)  $\sim t_{\text{ox}}(W \sim 42$  nm)  $\sim 322$  nm,  $t_{\text{ox}}(W \sim 68$  nm)  $\sim 305$  nm. (b)  $L$ -dependence of noise behavior of SLR3 ( $L \sim 0.61$   $\mu\text{m}$ ) and SLR4 ( $L \sim 1.13$   $\mu\text{m}$ ) with a similar width ( $W \sim 30$  nm) at  $T = 77$  K in scale of  $(V_g - V_{\text{Dirac}})^{1/2}$ . As  $L$  increases, the number of noise peaks (as arrowed) decreases, possibly because the disorder results in subband mixing. The inset shows the schematics of quasi-1D DOS in scale of  $(V_g - V_{\text{Dirac}})^{1/2}$ .

1b). Starting from a qualitative explanation, the correlation between the conductance fluctuations and the band structure of SLR can be viewed as follows: In the presence of trap states, the trapping/detrapping processes cause the fluctuations of Fermi energy ( $\Delta E_F$ ) that originate from the change of screened Coulomb potential of the traps. Consequently, the  $\Delta E_F$  induces enhanced conductance fluctuations near the threshold of the  $n$ th subband ( $E_n$ ), because the DOS ( $\rho_n(E) \propto (E - E_n)^{-1/2}$ ) diverges near  $E \sim E_n$ .<sup>27</sup> Correspondingly, the conductance fluctuations are suppressed between the thresholds of subbands where the profile of DOS is smoother. Our physical picture is consistent with the general noise model as referred in III–V quantum structures,  $S_V/V^2 = S_G/G^2 \propto (1/G^2)(\partial G/\partial E_F)^2$ , where  $S_G$  is the noise spectral density of the conductance fluctuations.<sup>12</sup> We note that the noise peaks disappear at 300 K and at higher gate biases, which mainly result from the subband mixing caused by the temperature and disorder (short-range), respectively.<sup>26,27</sup>

To quantify our explanation, we further study the dimension-dependence of the noise. Quantitative analysis shows that the noise peak is indeed a measure of the band structure as described below.

As  $W$  increases, the separation of noise peaks decreases (as arrowed in Figure 2a); this fact is consistent with the  $W$ -dependence of subband separations in SLR.<sup>23,26,27</sup> We apply the classical model of a conducting strip to estimate the gate capacitances as<sup>23,35</sup>  $C_g \sim C_c \sim 4.6 \times 10^{11}$   $\text{cm}^{-2}$   $\text{V}^{-1}$  ( $W \sim 42$  nm,  $t_{\text{ox}} \sim 322$  nm) and  $3.2 \times 10^{11}$   $\text{cm}^{-2}$   $\text{V}^{-1}$  ( $W \sim 68$  nm,  $t_{\text{ox}} \sim 305$  nm). Consequently, using the energy relation  $E = \hbar v_F(C_g \pi |V_g - V_{\text{Dirac}}|)^{1/2}$ , the measured noise peak separation (as arrowed) can be converted to be  $\Delta E \sim 82$

meV ( $W = 42$  nm) and 49 meV ( $W = 68$  nm). On the basis of the band structure, the subband separation is  $\Delta E_{\text{DOS}} \sim \pi \hbar v_F/W \sim 49$  meV ( $W = 42$  nm) and 30 meV ( $W = 68$  nm), respectively. The discrepancy between  $\Delta E$  and  $\Delta E_{\text{DOS}}$  (within a factor of 2) is due to the overestimation of  $C_g$ .<sup>23,35</sup> The ratio  $\Delta E_{\text{DOS}}(42$  nm)/ $\Delta E_{\text{DOS}}(68$  nm)  $\sim 1.62$  reasonably matches the ratio  $\Delta E(42$  nm)/ $\Delta E(68$  nm)  $\sim 1.68$  for the noise peak separations; this fact strengthens our statement that the noise peaks strongly correlate to the subband structures formed by the quantum confinement along the width.

As  $L$  increases, the number of noise peaks decreases (as arrowed in Figure 2b) because of the subband mixing resulting from an increase of disorder.

In Figure 2b, we also observe a series of seven noise peaks in SLR3 ( $W/L \sim 30$  nm/0.61  $\mu\text{m}$ ) that quantitatively follow the  $K$ – $K'$  subbands splitting in the DOS. That is, the noise peaks show alternative separations, giving  $\Delta E'/\Delta E \sim 0.29$  ( $\Delta E'$  is the  $K$ – $K'$  subband splitting), a ratio comparable to theoretical predictions for armchair nanoribbons (0.13–0.46).<sup>23,24</sup> The ratio  $\Delta E(30$  nm)/ $\Delta E(42$  nm)  $\sim 1.9$  ( $\Delta E(30$  nm) is estimated between the odd-order noise peaks) reasonably matches the ratio  $\Delta E_{\text{DOS}}(30$  nm)/ $\Delta E_{\text{DOS}}(42$  nm)  $\sim 1.4$ . This  $K$ – $K'$  subband splitting effect is not clearly observed in SLR1 and SLR2 (Figure 2a), where the splitting separation ( $\Delta E'$ ) can be smeared out by temperature. To prove this, we did measurement for SLR1 at  $T = 4.19$  K, where extra noise peaks (corresponding to the  $K$ – $K'$  subband splitting) are observed ( $\Delta E'/\Delta E \sim 0.4$ ) comparing with the case at 77 K (see Supporting Information).

While the noise peaks are well-defined by the quantum confinement along the width, we note that the ideal con-

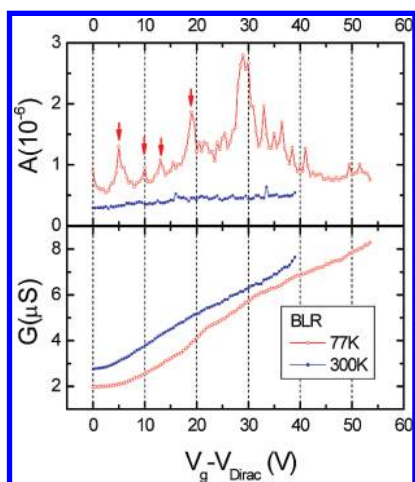


**FIGURE 3.** Temperature-dependence of noise behavior (and conductance) in bilayer graphene nanoribbon (BLR).  $T$ -dependence of noise behavior in BLR1 ( $W \sim 49$  nm,  $L \sim 0.79$   $\mu\text{m}$ ) is presented in scale of  $V_g - V_{\text{Dirac}}$ . At  $T = 77$  K, the noise peaks (as arrowed) appear while the corresponding conductance plateaus (bottom) are not obvious.

ductance plateaus can be significantly disturbed by disorders (see Figure 2a,b). For example, SLR2 ( $W \sim 68$  nm) shows lower conductance than that of SLR1 ( $W \sim 42$  nm), indicating a smaller transmission coefficient of subbands in SLR2 due to disorder.<sup>23,27</sup> Detailed AFM scanning shows that SLR2 is indeed more disordered (e.g., nonuniformity of width and chemical residual, see Supporting Information). The reason may be that while all disorders contribute to the scattering that disturb the conductance from the ideal case, only the trap states near the Fermi-energy (partial disorder) that cause the trapping-detrapping processes contribute to the measured noise. This fact suggests that the noise is a more direct probing mechanism for the subband structure of SLRs than the conductance.

Comparing with SLR, BLR has more complicated subband structures and the theoretical works on its fundamental transport are still rare.<sup>36,37</sup> We thus limit the discussion of BLR to be qualitative.

The main feature for BLR is that (see Figure 3) the noise peaks are apparent at  $T = 77$  K (smeared at 300 K), whereas the corresponding conductance plateaus are not as obvious. Also, BLR shows more noise peaks than SLR, and the noise peaks (as arrowed) are not equidistant in the scale of  $V_g - V_{\text{Dirac}}$ ; both facts are consistent with the BLR subband structure, where the separation of subbands is smaller than SLR and not equidistant in the energy scale.<sup>36</sup> Thus, similar to the discussions in SLR, we attribute these noise peaks in BLR to the enhanced conductance fluctuation near its subband thresholds. This fact reaffirms that the noise can act as a robust mechanism to directly probe the DOS, especially for BLR whose subband structures are smeared out in conductance measurement. Complicated by the subband structure, we did not see clear dimension-dependence of the noise peaks in BLR.<sup>38</sup> Besides, we note that the noise level

of BLR is overall lower than that of SLR with similar  $L$  and  $W$ , which may relate to the carrier screening effect in BLR.<sup>28</sup>

Finally, we discuss about the  $T$ -dependence of the noise behavior in our GNRs. In our measurement, no clear (or weak)  $T$ -dependence of conductance value is observed for both SLR and BLR (see Supporting Information), while the noise floor (other than the noise peaks) is larger at 77 K than 300 K (see Figures 1b and 3). This fact appears similar to the noise theorem in the hopping regime:<sup>39,40</sup> the noise increase at 77 K can come from the reduced number of conducting paths, thus the effective conducting area reduces and the noise ( $\sim 1/\text{Area}$ ) increases. Furthermore, we measured the large graphene ( $\sim$ micrometer width) and found an opposite  $T$ -dependence: the noise is lower at 77 K than 300 K (not shown). This suggests that the edge significantly impacts the noise behavior of GNRs, since edge states are more influential in GNR transport than large graphene.

In conclusion, we observe the enhanced conductance fluctuations in GNRs induced by the quantum confinement effect along the widths; this is clearly proved by the strong correlation between the noise peaks and the band structure (DOS) of the GNRs on the quantitative level. This correlation provides a robust mechanism to electrically probe the band structure of GNRs, especially when the subband feature is smeared out in the conductance ( $G$ ) measurement. Our result can extend to research in a broad range of low-dimensional nanostructures, which promotes the noise-based metrology for the electronic band structure of quantum transport systems.

**Acknowledgment.** The authors are thankful for helpful discussions with F. Miao, Y. Zhou, X. Zhang, and I. Ovchinnikov and experimental support from S. Aloni and T. Kuykendall. This work was in part supported by MARCO Focus Center on Functional Engineered Nano Architectonics and the U.S. Department of Energy under Contract No. DE-AC02-05CH11231.

**Supporting Information Available.** Methods, definition of the noise figure, AFM image of SLR1 and SLR2,  $K-K'$  subband splitting of SLR1 at  $T = 4.19$  K, weak temperature-dependence of conductance of SLR and BLR, additional references, and additional figures. This material is available free of charge via the Internet at <http://pubs.acs.org>.

## REFERENCES AND NOTES

- (1) Tsui, D. C.; et al. Two-dimensional magnetotransport in the extreme quantum limit. *Phys. Rev. Lett.* **1982**, *48*, 1559–1562.
- (2) Datta, S. *Electronic transport in mesoscopic systems*; Cambridge University Press: Cambridge, 2003.
- (3) Hsieh, D.; et al. Observation of unconventional quantum spin textures in topological insulators. *Science* **2009**, *323*, 919–922.
- (4) Staring, A. A. M.; et al. Coulomb-blockade oscillations in disordered quantum wires. *Phys. Rev. B* **1992**, *45*, 9222–9236.
- (5) Huibers, A. G.; et al. Dephasing in open quantum dots. *Phys. Rev. Lett.* **1998**, *81*, 200–203.
- (6) Cobden, D. H.; et al. Noise and reproducible structure in a GaAs/Al<sub>x</sub>Ga<sub>1-x</sub>As one-dimensional channel. *Phys. Rev. B* **1991**, *44*, 1938–1941(R).

- (7) Marcus, C. M.; et al. Conductance fluctuations and chaotic scattering in ballistic microstructures. *Phys. Rev. Lett.* **1992**, *69*, 506.
- (8) Nikolic, K.; MacKinnn, A. Conductance and conductance fluctuations of narrow disordered quantum wires. *Phys. Rev. B.* **1994**, *50*, 11008–11017.
- (9) Skvortsov, M. A.; Feigel'man, M. V. Superconductivity in disordered thin films: giant mesoscopic fluctuations. *Phys. Rev. Lett.* **2005**, *95*, No. 057002.
- (10) van Der Zeil, A. Unified presentation of  $1/f$  noise in electronic devices: fundamental  $1/f$  noise sources. *Proc. IEEE* **1988**, *76*, 235–258, No. 3.
- (11) Lin, Y. M.; et al. Low-frequency current fluctuations in individual semiconducting single-wall carbon nanotubes. *Nano Lett.* **2006**, *6*, 930–936.
- (12) Dekker, C.; et al. Spontaneous resistance switching and low-frequency noise in quantum point contacts. *Phys. Rev. Lett.* **1991**, *66*, 2148–2151.
- (13) Bezrukov, S. M.; Kasianowicz, J. J. Current noise reveals protonation kinetics and number of ionizable sites in an open protein ion channel. *Phys. Rev. Lett.* **1993**, *70*, 2352–2355.
- (14) Leturcq, R.; et al. Resistance noise scaling in a dilute two-dimensional hole system in GaAs. *Phys. Rev. Lett.* **2003**, *90*, No. 076402.
- (15) Buizert, C.; et al. In Situ reduction of charge noise in GaAs/Al<sub>x</sub>Ga<sub>1-x</sub>As Schottky-gated devices. *Phys. Rev. Lett.* **2008**, *101*, 226603.
- (16) Geim, A. K.; Novoselov, K. S. The rise of graphene. *Nat. Mater.* **2007**, *6*, 183–191.
- (17) Freitag, M.; et al. Thermal infrared emission from biased graphene. *Nat. Nanotechnol.* **2010**, *5*, 497–501.
- (18) Han, M. Y.; et al. Energy band-gap engineering of graphene nanoribbons. *Phys. Rev. Lett.* **2007**, *98*, 206805.
- (19) Sols, F.; et al. Coulomb blockade in graphene nanoribbons. *Phys. Rev. Lett.* **2007**, *99*, 166803.
- (20) Stampfer, C.; et al. Energy gaps in etched graphene nanoribbons. *Phys. Rev. Lett.* **2009**, *102*, No. 056403.
- (21) Gallagher, P.; et al. Disorder-induced gap behavior in graphene nanoribbons. *Phys. Rev. B.* **2010**, *81*, 115409.
- (22) Han, M. Y.; et al. Electron transport in disordered graphene nanoribbons. *Phys. Rev. Lett.* **2010**, *104*, No. 056801.
- (23) Lin, Y. M.; et al. Electrical observation of subband formation in graphene nanoribbons. *Phys. Rev. B.* **2008**, *78*, 161409(R).
- (24) Lian, C.; et al. Quantum transport in graphene nanoribbons patterned by metal masks. *Appl. Phys. Lett.* **2010**, *96*, 103109.
- (25) García-Mochales, P.; et al. Conductance in disordered nanowires: forward and backscattering. *Phys. Rev. B* **1996**, *53*, 10268–10280.
- (26) Mucciolo, E. R.; et al. Conductance quantization and transport gaps in disordered graphene nanoribbons. *Phys. Rev. B.* **2009**, *79*, No. 075407.
- (27) Ihnatsenka, S.; Kirczenow, G. Conductance quantization in strongly disordered graphene ribbons. *Phys. Rev. B.* **2009**, *80*, 201407(R).
- (28) Lin, Y. M.; Avouris, P. Strong suppression of electrical noise in bilayer graphene nanodevices. *Nano Lett.* **2008**, *8*, 2119–2125.
- (29) Bai, J.; et al. Rational fabrication of graphene nanoribbons using a nanowire etch mask. *Nano Lett.* **2009**, *9*, 2083–2087.
- (30) Tobias, D.; et al. Origins of  $1/f$  noise in individual semiconducting carbon nanotube field-effect transistors. *Phys. Rev. B.* **2008**, *77*, No. 033407.
- (31) This definition helps to reduce the measurement errors of the noise at specific frequencies, and rule out other types of noise sources (e.g. thermal noise, ac electricity power noise, etc.).
- (32) Lee, E. J. H.; et al. Contact and edge effects in graphene devices. *Nat. Nanotechnol.* **2008**, *3*, 486–490.
- (33) Yuan, J.; et al. Observation of anomalous phonon softening in bilayer graphene. *Phys. Rev. Lett.* **2008**, *101*, 136804.
- (34) Yu, Y. J.; et al. Tuning the graphene work function by electric field effect. *Nano Lett.* **2009**, *9*, 3430–3434.
- (35) Shylau, A. A.; et al. Capacitance of graphene nanoribbons. *Phys. Rev. B* **2009**, *80*, 205402.
- (36) Xu, H.; et al. Edge disorder and localization regimes in bilayer graphene nanoribbons. *Phys. Rev. B* **2009**, *80*, No. 045308.
- (37) Li, X.; et al. Pseudospin valve in bilayer graphene nanoribbons. *Phys. Rev. B* **2010**, *81*, 195402.
- (38) Other possible reasons such as the gate-induced bandgap-opening effect (see ref 36) may also cause the change of the subband structures, and thus the position of noise peaks in BLR. However, experimental evidence of this bandgap-opening effect in BLR is still lacking.
- (39) Kozub, V. I. Low-frequency noise due to site energy fluctuations in hopping conductivity. *Solid State Commun.* **1996**, *97*, 843–846.
- (40) Shklovskii, B. I.  $1/f$  noise in variable range hopping conduction. *Phys. Rev. B* **2003**, *67*, No. 045201.